Assiut University Journal of Multidisciplinary Scientific Research (AUNJMSR)
Faculty of Science, Assiut University, Assiut, Egypt.
Printed ISSN 2812-5029
Online ISSN 2812-5037
Vol. 54(1): 130- 142 (2025)
https://aunj.journals.ekb.eg

Nanosized Aluminum Metal-Organic Framework Encapsulating Edaravone Drug: Synthesis and Characterization.

Rabab M. Thabit [1], A. Abu El-Fadl [1], A. A. Abu-Sehly [1] and Ahmed M. Sayed [2,*]

[1] Faculty of Science, Physics Department, Assiut University, 71516 Assiut, Egypt
[2] Faculty of Science, Chemistry Department, Assiut University, 71516 Assiut, Egypt
[*]Ahmed M. Sayed: ahmed.sayed@aun.edu.eg

ARTICLE INFO
Article History:
Received: 2024-10-23
Accepted: 2024-11-24
Online: 2024-12-26

Keywords:
Metal-organic framework, Edaravone, UV-VIS, EE, LC, TEM, FTIR, XRD, TGA.

ABSTRACT

The solvothermal method was employed to synthesize nanoporous aluminum metal-organic framework (Al-MOF) nanoparticles (NPs), which were utilized as a matrix for the pharmaceutical delivery of Edaravone (Ed). The drug encapsulation efficiency (EE) and loading capacity (LC) percents indicate the potential of Al-MOF NPs as effective drug delivery vehicles, where found to be 60% and 12% respectivly. The structural and functional properties of both the Al-MOF NPs and Ed-loaded Al-MOF NPs (Ed@Al-MOF) were characterized using several techniques, including ultraviolet-visible (UV-Vis) spectroscopy, Transmission Electron Microscopy (TEM) for morphological analysis, X-ray diffractometry (XRD), and Fourier-transform infrared (FTIR) spectroscopy and all show successfully synthesized of Ed@Al-MOF NPs composite. Additionally, the thermal stability of the Ed@Al-MOF NPs was evaluated through thermogravimetric analysis (TGA) that exhibit good thermal stability . These promising results underscore the potential of Al-MOF NPs as a viable platform for drug delivery, necessitating further investigations to confirm the applicability of Ed@Al-MOF NPs in therapeutic contexts.

1. INTRODUCTION

Nanomaterials have the potential to alter the functions of materials at various scales. Metal-organic frameworks (MOFs) can be described as hybrid materials [1, 2]. MOFs known as porous coordination polymers (PCPs), are crystalline, materials made of metal clusters or ions connected by organic linkers. Also, MOFs offer molecular-

structural control, tunable porosity, varied chemical structures, and advanced surface characteristics [3].

MOFs were first described in 1989 as coordination networks with possible porosity [4-6]. MOFs were developed as task-specific materials in the 1990s, using different functional groups to control their geometry and size [7, 8]. The process of reticular synthesis creates inorganic-organic crystalline frameworks that can be modified with metal nodes and organic linkers.[9, 10] Moreover, the choice of MOF components can give extremely high porosity, and the functions of MOFs may be demonstrated by chemical components used in the backbone [11-14].

Using a variety of techniques, including diffusion, hydrothermal (solvothermal), microwave, and electrochemical procedures, the synthesis of MOFs has been extensively developed. Post-synthetic alterations of MOFs, on the other hand, are helpful for adding further capabilities [15, 16]. The range of potential biological uses for metal-organic frameworks (MOFs) has expanded due to their industrial applications in gas storage, catalysis, gas adsorption, separations, nonlinear optics, and sensing [3, 8],[17-20]. Because of their unique features, nanoscale MOFs received a lot of interest for use in drug delivery systems (DDSs) for tumor therapy. For this reason, characteristics like high porosity and surface area are useful for increasing drug loading efficiency, but they can also increase bioavailability. Other benefits include strong tenability, good biocompatibility, water solubility, and biodegradability [21]. These features allow them to load and release a variety of cargos, including medicinal medicines. Férey and coworkers argued in 2006 that MOFs have potential in drug delivery due to their high loading capacities and regulated release behavior [22].

The selection of stable, ecologically safe MOFs with strong adsorption properties is crucial. As a result, consideration has progressively shifted to light and non-toxic metal elements including magnesium [23, 24], calcium [25, 26], and aluminum [27, 28]. when choosing metal ions for the synthesis of MOFs.

Aluminum makes up 8.3% of the earth's crust by weight and is a more common, affordable, and non-toxic metal [28]. The connecting of aluminium-centered octahedra can form inorganic sub-networks of Al-MOF NPs [29-31]. The aluminum's octahedral coordination and strong bonds Al–O give exceptional hydrothermal stability [30, 31]. Al-

MOF NPs have extremely research in both industry and biology [29-31]. These characteristics result in many research used the distinct characteristics of Al-MOF NPs in different fields.

As a free radical scavenger, Edaravone (3-methyl-1-phenyl-2-pyrazolin-5-one) (Ed) exhibits strong antioxidative properties, primarily through the removal of hydroxyl radicals and the inhibition of lipid peroxidation [32]. Edaravone was initially licensed to be a cerebroprotective drug to treat acute ischemic stroke in a few countries, such as Japan, China, and India. It does this by shielding neuronal cells from oxidative damage and preventing cerebral edema [33, 34]. The use of Edaravone as a medication to stop the fatal neurodegenerative disease amyotrophic lateral sclerosis (ALS) has also been expanded in several nations [35, 36]. Edaravone's strong neuroprotective properties against ischemic stroke and ALS, various nations are conducting more clinical studies to expand the drug's use [37, 38].

Ed was effectively loaded into Al-MOF NPs in this research to assess their encapsulation efficiency (EE) and loading capacity (LC) percents. The Morphological features of Al-MOF NPs were investigated by Transmission Electron Microscopy (TEM). Moreover, structural and functional features were characterized by ultraviolet-visible spectrum (UV-Vis), Fourier-transformed infrared spectroscopy (FTIR), X-ray diffractometry (XRD), and thermal gravimetric analysis (TGA).

2. MATERIALS AND METHODS

2.1. Materials

Ed, Aluminium Nitrate Nonahydrate ($Al(No_3)_3 \cdot 9H_2O$, 98%), Dimethylformamide (DMF, 98%), Organic linker 1,4-benzene dicarboxylate (BDC) and Ethanol (C_2H_6O, .95%) were purchased from (Sigma).

2.2. Synthesis of Aluminum MOF NPs and Edaravone loading

The Al-MOF NPs were synthesized utilizing a solvothermal approach in a steel pressure vessel, showed as in scheme 1. The employed sources, were metal salt and organic linkers, were combined directly into a solvent, DMF was used as the solvent, and the reaction was carried out at temperatures above several hundred degrees Celsius (in Teflon-lined stainless-steel autoclave). Crystals develop under autogenous pressure. The

autoclaves require thick steel that can endure high pressures and temperatures for a long time throughout the synthesis process [39]. To create Ed@Al-MOF NPs, A solution of Ed ethanol-water was mixed with a one-milliliter solution of ethanol-water of Al-MOF. The Ed@Al-MOF NPs were then centrifuged at around 8000 rpm for 30 minutes.

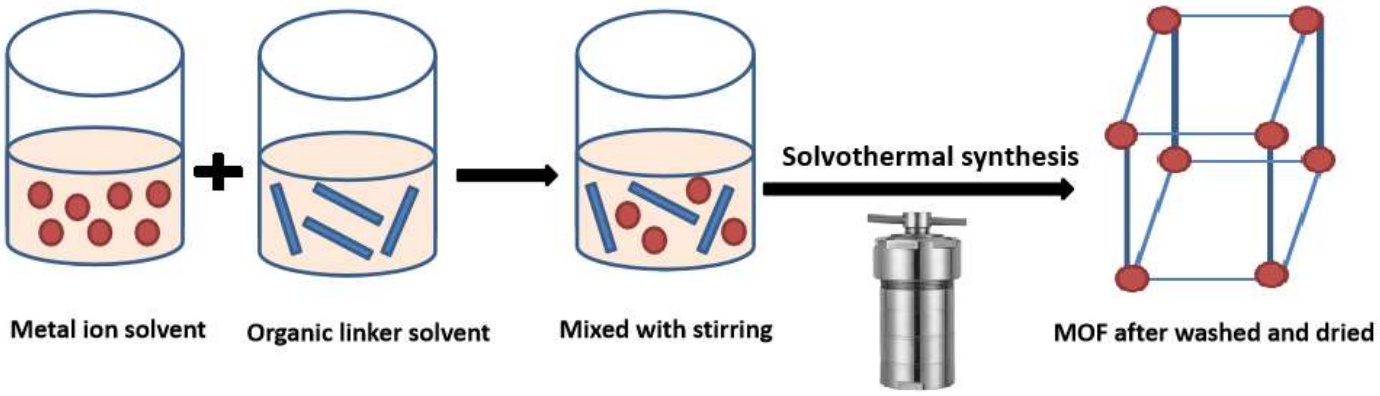

Scheme 1. Metal organic framework (MOF) solvothermal synthesis method.

2.3. Characterization of Al-MOF NPs and Ed @Al-MOF NPs composites.

2.3.1. Drug loading capacity (LC) and drug entrapment efficiency (EE) percentage measurement.

By extracting Ed@Al-MOF NPs, after centrifuging composite from an aqueous media containing free drug for 30 minutes at surrounding temperature at 8,000 rpm, the LC and EE of Al-MOF for Ed were investigated. The amount of free Ed was measured using a UV spectrophotometer adjusted to 238 nm in relation to the standard Ed curve.

$$\mathrm{LC}(\%) = \frac{total\ amount\ of\ Ed - free\ Ed}{nanoparticles\ weight} x100\% \quad (1)$$

$$\mathrm{EE}(\%) = \frac{total\ amount\ of\ Ed - free\ Ed}{total\ amount\ of\ Ed} x100\% \quad (2)$$

Using the above formulas (1) and (2), to determine the process loading Ed's LC and EE.

2.3.2. Transmission Electron Microscopy (TEM)

The morphological characteristics of the samples were analyzed using a JEOL 2100 transmission electron microscope (TEM). The samples were prepared by dissolving them in ethanol, followed by 10 minutes of sonication. Afterward, they were placed onto copper grids and allowed to air dry at room temperature. Once the samples had completely dried, digital micrographs were captured and analyzed using specialized software, including Digital Micrograph and Soft Imaging Viewer, to assess their structural features.

2.3.3. X-ray diffractometry (XRD)

XRD patterns of Ed, Al-MOF NPs, and Ed@Al-MOF NPs were obtained using a Philips XRD PW 1710 control unit (Holland). The samples were scanned with high-intensity Cu Kα X-radiation (λ = 1.5405 Å) that was graphite monochromatized. The system operated at 40 kV and 30 mA, with a 2θ scanning range from 4° to 80° and a step size of 0.06°. These conditions allowed for precise identification of the crystalline structure of the samples

2.3.4. Fourier Transform Infrared Spectroscopy (FT-IR)

The FT-IR spectra of Ed, Al-MOF, and Ed@Al-MOF NPs were recorded using a Thermo Scientific FT-IR spectrophotometer (USA) equipped with a smart OMNI-sampler accessory. The analysis was conducted in the wavenumber range of 400–4000 cm^{-1}. For each sample, pelletized discs were prepared by mixing 2 mg of the material with 10 mg of potassium bromide (KBr), and the spectra were collected to identify characteristic functional groups and molecular interactions.

2.3.5. Thermal gravimetric analysis (TGA)

TGA was used to characterize the specimens. The study was conducted using a Shimadzu DTG-60H simultaneous DTA-TG apparatus under an air-filled environment. The analysis covered a temperature range of 50 to 800 °C, with a heating rate of 10 °C per minute, while maintaining an air flow rate of 40 mL per minute. This approach allowed for the precise assessment of thermal stability and weight loss of the materials as a function of temperature.

3. RESULTS AND DISCUSSIONS

3.1. Drug loading capacity (LC) and drug entrapment efficiency (EE) percents of Al-MOF

The LC and EE of the Ed@Al-MOF NPs composite were determined to be 12% and 60%, respectively, using a UV spectrophotometer (PE, USA) calibrated at 238 nm. These values highlight the capability of Al-MOF NPs as an effective drug delivery system, offering significant drug loading and efficient encapsulation of therapeutic agents. The measured LC and EE reflect the composite's potential for targeted drug delivery applications, enabling controlled release and improved therapeutic outcomes.

3.2. Transmission Electron Microscopy (TEM)

Figure 1 presents TEM images of both Ed@Al-MOF and Al-MOF nanoparticles. In Figure. 1a, the Al-MOF nanoparticles exhibit a smooth, light spherical morphology with a size around 73.71nm, appearing grey in the image. In contrast, Figure. 1b shows Ed@Al-MOF NPs, which maintain a similar size of approximately 73.71nm but appear more aggregated and darker, indicating the successful encapsulation of Edaravone (Ed) within the Al-MOF nanoparticles, as well as potential changes in surface characteristics after drug loading.

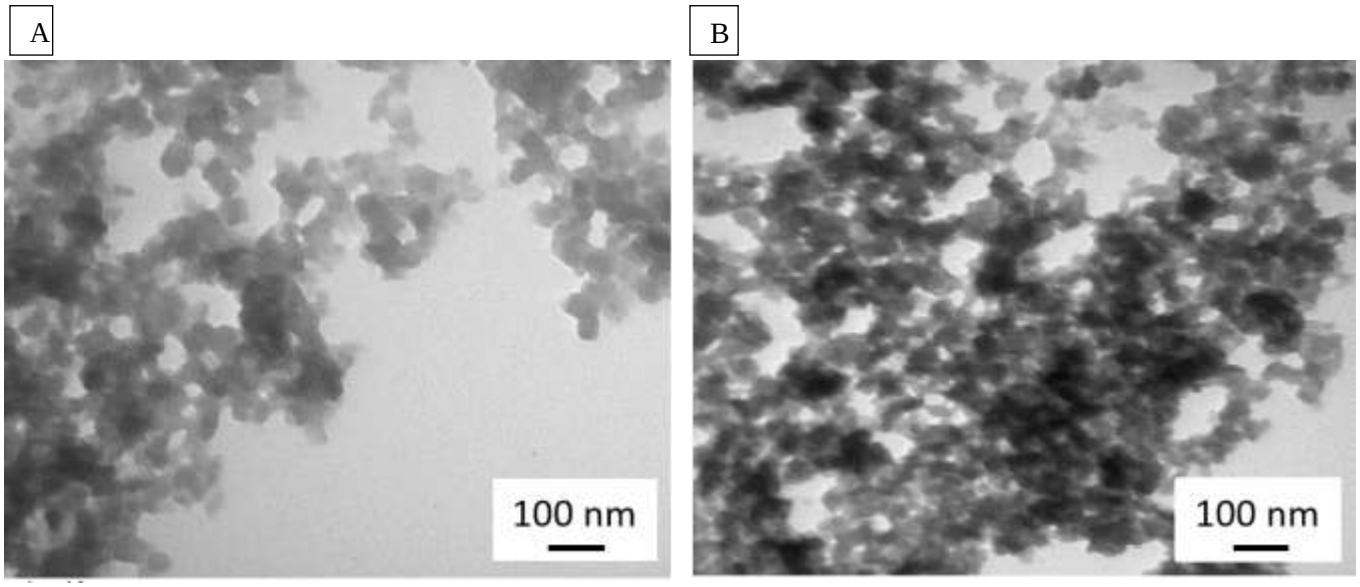

Figure 1. Representative Transmission Electron Microscopy (TEM) images of (a) Al-MOF NPs, (b) Ed-loaded Al-MOF NPs composites synthesized.

3.3. X-ray Diffractometry (XRD)

Figure 2 presents the XRD patterns of Al-MOF NPs, Ed, and the composite Ed@Al-MOF NPs. In the XRD pattern of pure Ed, three prominent diffraction peaks at 2θ values of 11.2°, 14.0°, and 21.4° confirm its crystalline nature [40]. The Al-MOF NPs exhibit diffraction peaks at 2θ values of 8.68° and 17.68°, consistent with previously reported crystalline structures of Al-MOF [41,42]. Upon loading Ed into Al-MOF, the XRD pattern of Ed@Al-MOF NPs shows additional peaks at 12.4° and enhanced intensities at 8.38°, 14.74°, and 17.62°, as well as new peaks at 9.7° and 20.26°, providing evidence of successful drug loading.

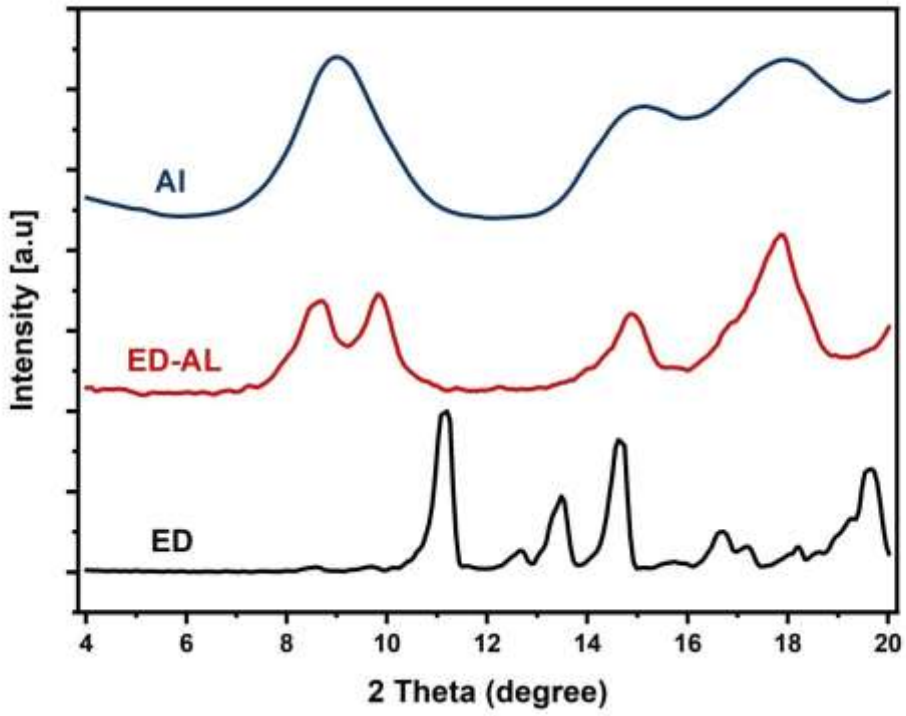

Figure 2. X-ray diffraction patterns (XRD) patterns of Al MOF NPs, Ed and Ed-loaded Al MOF-NPs synthesized composites.

A typical way to present the particle size and its distribution is in the form of a number-frequency histogram. A histogram is a bar graph that illustrates the frequency of occurrence versus the size range. Figure 3 shows number frequency histograms of

particle size data in linear scale. The smooth curve drawn through the histogram gives the average value of the size. The particle characteristics data obtained on Ed@Al-Mof nanoparticles is indicated in Figure 3 is 73.71 nm.

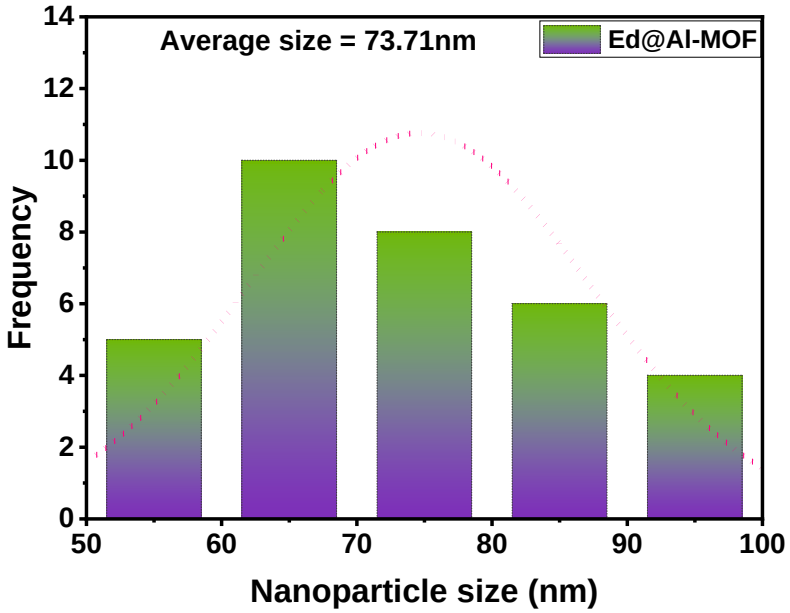

Figure 3 . shows the grain size distribution of Ed@Al-Mof nanoparticles by using the histogram.

3.4. Fourier Transform Infrared Spectroscopy (FT-IR)

The FT-IR of Al-MOF NPs, Ed and Ed@Al-MOF spectra are shown in Figure 4. In the Edaravone FTIR spectra, the characteristic C=O stretching peak of the carbonyl group was detected at about 1800 cm^{-1}. Nevertheless, as observed in Edaravone, the characteristic peaks for C=O stretching and hydroxyl group, are similar to previous observations in [40, 43]. Figure 4 displays the FTIR spectra of the Al-MOF NPs shows the carboxylic functional group of the Al-MOF NPs exhibits vibration bands in the range of 1,400–1,700 cm^{-1}. Furthermore, asymmetric stretching (-COO-) is shown by bands at 1,608 and 1,512 cm^{-1}, whereas symmetric stretching (-COO-) is indicated by bands at 1,435 and 1,417 cm^{-1}. Additionally, the absorption band at 1,669 cm^{-1} was formed by the -COOH group of unreacted BDC molecules being trapped in the cavities of Al-MOF NPs in accordance with previously published results [41]. The Ed@Al-MOF NPs ' spectra displayed shifts at various peaks, and the characteristic Ed peaks vanished from the Al-

MOF NPs' spectrum. This suggests that Ed particles were on the surface of the Al NPs rather impeded within Al NPs matrix, and it may have revealed a conjugation between Ed and Al-MOF NPs.

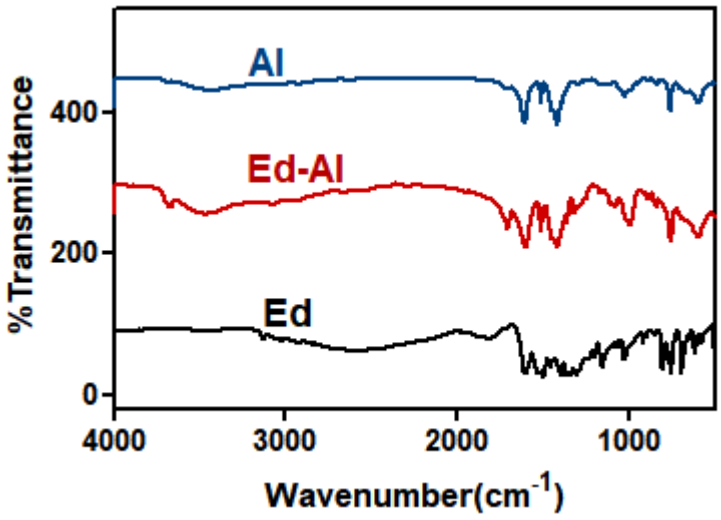

Figure 4. Fourier Transform Infrared Spectroscopy (FTIR) spectra of (a) Al-MOF NPs, (b) Ed-loaded Al-MOF NPs synthesized composites and (c) Ed drug.

3.5. Thermal Gravimetric Analysis (TGA)

TGA was employed to assess the mass loss of Ed loaded into Al-MOF NPs. The complex was heated from 50 to 600 °C under an airflow of 40 ml/min at a steady heating rate of 10 °C/min. As illustrated in Figure 5, the TGA profile of Ed@Al-MOF NPs demonstrated a weight loss 56% within the temperature range of 120.51–569.5 °C. This weight loss corresponds to the thermal degradation of the Ed-loaded Al-MOF NPs conjugate, as well as the evaporation of adsorbed water. These results confirm that the synthesized Ed@Al-MOF NPs exhibit good thermal stability.

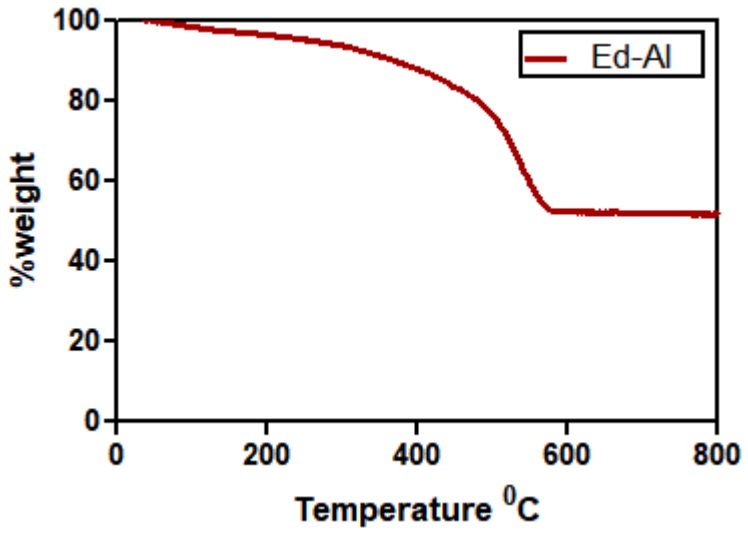

Figure 5. Thermogravimetric analysis (TGA) profile of Ed loaded Al-MOF NPs synthesized complex.

4. CONCLUSION

In this study, we successfully synthesized Al-MOF and Ed@Al-MOF NPs using a hydrothermal method. The EE% and LC% of Ed in the Al-MOF NPs were found to be substantial, demonstrating their potential as drug carriers. Multiple characterization techniques confirmed the successful loading of Ed into the Al-MOF NPs. TEM analysis revealed the nanoscale structure, while Rietveld refinement of XRD data identified the crystalline phases of both Al-MOF and Ed@Al-MOF NPs. FTIR spectra confirmed the structure of the Al-MOF and Ed, and the incorboration of Ed into the NPs composite. Additionally, TGA revealed the thermal stability of the Ed@Al-MOF NPs. These findings highlight the potential of Ed@Al-MOF NPs as effective platforms for biomedical applications. Further studies are necessary to validate their use in therapeutic settings.

REFERENCES

[1] S. Tran, P. J. DeGiovanni, B. Piel and P. Rai, Clin. Transl. Med., 2017, 6, 44.

[2] Z. Luo, S. Fan, C. Gu, W. Liu, J. Chen, B. Li and J. Liu, Curr. Med. Chem., 2019, 26, 3341.

[3] R. Freund, U. Lächelt, T. Gruber, B. Rühle, S. Wuttke, ACS Nano 2018, 12, 2094.

[4] B. F. Hoskins, R. Robson, J. Am. Chem. Soc. 1989, 111, 5962.

[5] R. S. Forgan, Chem. Sci. 2020, 11, 4546.

[6] A. Schneemann, V. Bon, I. Schwedler, I. Senkovska, S. Kaskel, R. A. Fischer, Chem. Soc. Rev. 2014, 43, 6062.

[7] C. Vaitsis, G. Sourkouni, C. Argirusis, Ultrasonics Sonochem. 2019, 52, 106.

[8] O. M. Yaghi, M. O. Keeffe, N. W. Ockwig, H. K. Chae, M. Eddaoudi, J. Kim, Nature 2003, 423, 705.

[9] S. Yuan, J. S. Qin, C. T. Lollar, H. C. Zhou, ACS Cent. Sci. 2018, 4, 440.

[10] A. E. Baumann, D. A. Burns, B. Liu, V. S. Thoi, Commun. Chem. 2019, 2, 86.

[11] H. C. Zhou, J. R. Long, O. M. Yaghi, Chem. Rev. 2012, 112, 673.

[12] C. Gropp, S. Canossa, S. Wuttke, F. Gándara, Q. Li, L. Gagliardi, O. M. Yaghi, ACS Cent. Sci. 2020, 6, 1255.

[13] Z. Ji, H. Wang, S. Canossa, S. Wuttke, O. M. Yaghi, Adv. Funct. Mater. 2020, 30, 2000238.

[14] R. S. Forgan, Dalton Trans. 2019, 48, 9037.

[15] R. J. Marshall, R. S. Forgan, Eur. J. Inorg. Chem. 2016, 27, 4310.

[16] V. F. Samanidou, E. A. Deliyanni, Molecules 2020, 25, 960.

[17] I. Kurzydym, I. Czekaj, Tech. Trans. 2020, e2020012.

[18] T. Chalati, P. Horcajada, P. Couvreur, C. Serre, M. B. Yahia, G. Maurin, R. Gref, Nanomedicine 2011, 6, 1683.

[19] S. Mangal, S. S. Priya, MRS Energy Sustain. 2020, 38, 169.

[20] P. Silva, S. M. F. Vilela, J. P. C. Tomé, F. A. Almeida Paz, Chem. Soc. Rev. 2015, 44, 6774.

[21] Y. Wang, J. Yan, N. Wen, H. Xiong, S. Cai, Q. He, Y. Hu, D. Peng, Z. Liu, Y. Liu, Biomaterials 2020, 230, 119619.

[22] P. Horcajada, C. Serre, M. Vallet-Regí, M. Sebban, F. Taulelle, G. Férey, Angew. Chem. 2006, 118, 6120.

[23] S.-Q. Yang, F.-Z. Sun, P. Liu, L. Li, R. Krishna, Y.-H. Zhang, Q. Li, L. Zhou, T.- L. Hu, ACS Appl. Mater. Interfaces 2021, 13, 962.

[24] N. Wang, A. Mundstock, Y. Liu, A. Huang, J. Caro, Chem. Eng. Sci. 2015, 124 27.

[25] F. Hu, Z. Di, M. Wu, J. Li, Dalton Trans. 2020, 49, 8836.

[26] S. Xian, Y. Lin, H. Wang, J. Li, Small 2021, 17, 2005165.

[27] S. Biswas, T. Ahnfeldt, N. Stock, Inorg. Chem. 2011, 50, 9518.

[28] T. Loiseau, C. Volkringer, M. Haouas, F. Taulelle, G. F´erey, C. R. Chimie 2015, 18, 1350.

[29] M., Gaab, et al., The progression of Al-based metal-organic frameworks–From academic research to industrial production and applications. 2012, 157, 131.

[30] W., Fan, et al., Aluminum metal–organic frameworks: From structures to applications. 2023, 489, 215175.

[31] Stock, N.J.E.o.I. and B. Chemistry, Metal- organic frameworks: aluminium- based frameworks. 2011, 1.

[32] K. Watanabe, M. Tanaka, S. Yuki, M. Hirai, Y. Yamamoto, How is edaravone effective against acute ischemic stroke and amyotrophic lateral sclerosis? J. Clin. Biochem. Nutr. 2018, 62, 20.

[33] W. Müllges, D. Franke, W. Reents, J. Babin-Ebell, K. V. Toyka, N. Ko, S. Johnston, W. Young, V. Singh, A. Klatsky, Effect of a novel free radical scavenger, Edaravone (MCI-186), on acute brain infarction. Cerebrovasc. Dis. 2003, 15, 222.

[34] T. Fukuta, N. Oku, K. Kogure, Application and Utility of Liposomal Neuroprotective Agents and Biomimetic Nanoparticles for the Treatment of Ischemic Stroke. Pharmaceutics 2022, 14, 361.

[35] H. Houzen, T. Kano, K. Horiuchi, M. Wakita, A. Nagai, I. Yabe, Improved Long-Term Survival with Edaravone Therapy in Patients with Amyotrophic Lateral Sclerosis: A Retrospective Single Center Study in Japan. Pharmaceuticals (Basel) 2021, 14, 705.

[36] J. Rothstein, D. Edaravone: A new drug approved for ALS. Cell 2017, 171, 725.

[37] M. Fidalgo, J. Ricardo Pires, I. Viseu, P. Magalhaes, H. Gregorio, V. Afreixo, T. Gregorio, Edaravone for acute ischemic stroke - Systematic review with meta-analysis. Clin. Neurol. Neurosurg. 2022, 219, 107299.

[38] X. Xu, D. Shen, Y. Gao, Q. Zhou, Y. Ni, H. Meng, H. Shi, W. Le, S. Chen, S. Chen, A perspective on therapies for amyotrophiclateral sclerosis: can disease progression be curbed? Transl. Neuro degener. 2021, 10, 29.

[39] H. Reinsch , B. Marszałek , J. Wack , J. Senker , B. Gil , N. Stock : A new Al-MOF based on a unique column-shaped inorganic building unit exhibiting strongly hydrophilic sorption behaviour. Chemical communications 2012, 48, 9486.

[40] A. Parikh, K. Kathawala, C. C. Tan, S. Garg, & X. F. Zhou, Self-nanomicellizing solid dispersion of edaravone: Part I–Oral bioavailability improvement. Drug design, development and therapy 2018, 2051

[41] L. Yang, et al., Cu, Al and Ga based metal organic framework catalysts for the decarboxylation of oleic acid. Catalysis science & technology 2015, 5, 2777.

[42] R. M. Thabit, F. E. Z. A. A. El-Aziz, A. A. El-Fadl, , A. A. Abu-Sehly, & A. M. Sayed, Synthesis and evaluation of nanosized aluminum MOF encapsulating Umbelliferon: assessing antioxidant, anti-inflammatory, and wound healing potential in an earthworm model. BMC biotechnology, 2028, 24, 61.

[43] P. Rallapalli, et al., Sorption studies of CO 2, CH 4, N 2, CO, O 2 and Ar on nanoporous aluminum terephthalate [MIL-53 (Al)]. Journal of porous materials 2011, 18, 205.